

Reliability of Lead-Free LGAs and BGAs: Effects of Solder Joint Size, Cyclic Strain and Microstructure

Denis Barbini Ph.D. & Michael Meilunas
Universal Instruments Corporation
Conklin, NY, USA
barbini@uic.com

ABSTRACT

An accelerated thermal cycle experiment comparing similarly constructed area array devices representing Land Grid Array (LGA) and Ball Grid Array (BGA) technology with 0.254, 0.30, and 0.40mm diameter SAC305 solder balls was performed. The devices were subjected to three thermal cycle conditions in order to promote 2nd level solder fatigue. Failure data was compared using Weibull analyses. The results show that time to failure is highly influenced by the package pitch and thermal cycle temperatures in a manner predicted by simple mechanics. However, there were instances in which the effect of solder ball size did not fit the traditional solder joint reliability model in which increasing solder joint standoff height improves reliability (i.e. more cycles to failure). A theory is proposed that substantial differences in SAC305 solder joint Sn grain morphology may explain, at least partially, the discrepancies and evidence to support this theory is presented.

Key words: Land Grid Array (LGA), Ball Grid Array (BGA), SAC305, Accelerated Thermal Cycle (ATC)

INTRODUCTION

Many factors affect solder joint performance in accelerated thermal cycle (ATC) testing. The experiment described in this paper was designed to address three factors which are known to have substantial influence on solder joint fatigue times due to their effects on cyclic shear strain. These factors are solder ball size, solder joint distance from the neutral point (DNP), and accelerated thermal cycle operating temperatures.

Solder joint reliability is proportional to the in-plane shear strain which is cyclically accumulated and relieved during ATC testing. In its simplest form the maximum shear strain of a solder joint can be approximated by the equation:

$$\text{Equation 1. } \textit{strain} = \frac{DNP * \Delta\alpha * \Delta T}{h}$$

Where DNP is the solder joint's distance from the neutral point, $\Delta\alpha$ is the difference between the package body's coefficient of thermal expansion (CTE) and that of the printed circuit board, ΔT is the accelerated thermal cycle's cyclic temperature change, and h is the standoff height of the solder joint.

It is recognized that Equation 1 is often a gross overestimate of actual solder joint shear strain because the solder alloy has some resistance to deformation (i.e. stress accumulates) and because many surface mount technologies such as BGA and LGA have multiple I/Os which affect the distribution of the loading stress.

Equation 1 also fails to account for out-of plane stresses, which are usually associated with package warpage and which can be quite damaging to solder joints. However, regardless of its shortcomings, Equation 1 shows that increasing DNP, increasing ΔT and/or decreasing standoff height results in an increase in maximum shear strain which ultimately leads to a reduction in ATC lifetime.

BACKGROUND

Previously, the authors performed an ATC reliability analysis using three dummy SAC305 BGA and three dummy SAC305 LGA packages (23, 27, and 35mm body sizes). The devices were purchased from a single supplier and the LGAs were nothing more than the BGA components without pre-attached solder spheres. The samples were soldered to identical motherboards using the same solder paste and identical assembly practices. Solder joint standoff heights were measured and it was determined that the BGA standoff height was approximately 6.2 times greater than the LGA standoff height.

The assemblies were subjected to -40 to 125°C temperature cycling with 60 minute dwell times and were monitored in-situ using event detection. The test results were quite surprising. The data collected from the event detection system showed that the LGA packages, with an average solder joint standoff height of just 0.047mm, survived significantly more thermal cycles

than the comparable BGAs, which had 0.293mm solder joint heights. The results of the test, in Weibull plot form, are provided in Figure 1.

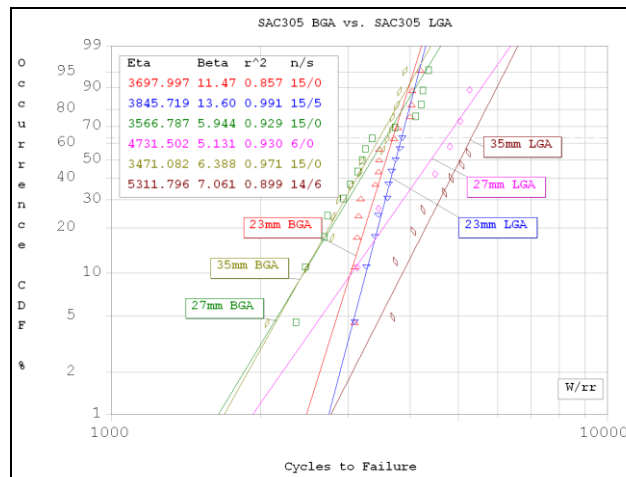


Figure 1. Weibull plots comparing SAC305 BGA solder joint reliability to SAC305 LGA solder joint reliability. Samples were tested using -40/125°C temperature cycling.

Failure analysis was performed on several samples after ATC testing. The selected samples were cross-sectioned into the solder joints which had been identified as electrically open. The solder joints were inspected using an optical microscope equipped with cross-polarized lenses. Examination revealed that the joints had failed due to solder fatigue, which was expected. But it was also noted that the microstructure of the LGA solder joints was significantly different from the microstructure of the BGA joints.

As shown in Figure 2, the LGA solder joints usually contained an interlaced twinned Sn grain morphology while the BGA solder joints were most often single grain or beach ball in appearance (Figure 3).

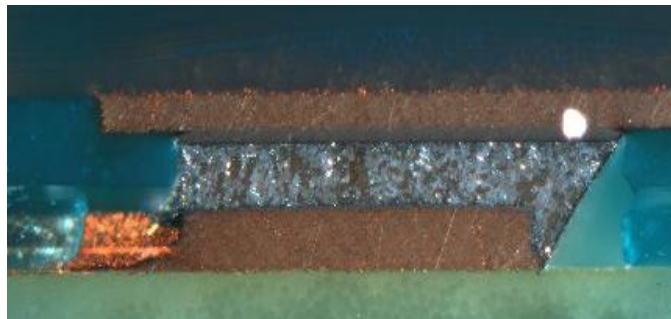


Figure 2. Cross polarized view of an LGA solder joint showing interlaced twinning Sn morphology.

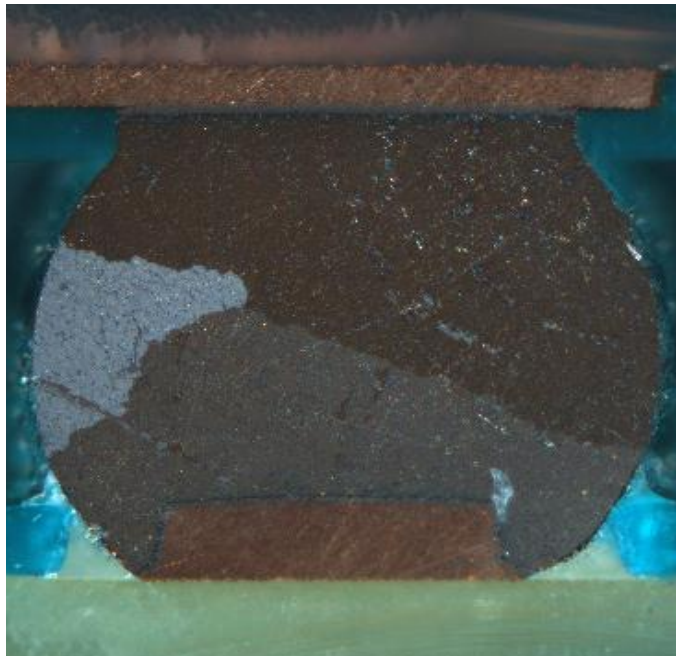


Figure 3. Cross polarized view of a BGA solder joint with the so-called 'beach ball' Sn grain morphology.

The fact that the Sn grain morphology of the SAC305 alloy was different for the two solder ball sizes was not surprising for numerous papers have been published regarding the various SAC305 microstructures including [1, 2, 3, 4, 5, 6, 7]. Some of these papers suggest that the interlaced twinned grain structure, which is most often associated with relatively small solder joints, have properties that inhibit thermal and mechanical fatigue processes. But direct comparisons between the reliability of the small solder joints and that of the larger joints are not readily available.

Instead, in papers such as [8], evidence is presented suggesting that smaller SAC305 solder joints fatigue at slower rates than large SAC305 solder joints subjected to the same strain or strain rate. But the smaller joints fail sooner (i.e. fewer cycles to failure) than the larger joints in these comparisons simply because they are soldered to smaller attachment pads on both the component and PCB. In our background experiment the BGA and LGA solder joints had identical pad sizes on the component and nearly identical pad sizes on the PCB, so the findings from [8] indicate that the smaller LGA solder joints could in fact survive more thermal cycles than the BGA solder joints.

TEST PLAN

Given that the printed circuit boards, assembly process, component bodies and test procedures described previously were identical, the logical assumption was that the differences between the solder joint microstructures most likely explains why the LGA survived more thermal cycles than the BGA. So a test plan was developed to determine if SAC305 LGAs containing interlaced twinned Sn grain morphology could perform better than SAC305 BGAs with beach ball Sn grain morphology for multiple strain states and ATC test temperatures.

To do so, identical components were manufactured with three different solder ball sizes in order to provide LGA and BGA style components with significantly different solder joint standoff heights. Five component pitches were incorporated into the test to investigate different solder joint stress/strain states ranging from very low (thousands of thermal cycles required for failure) to very high (only a few hundred thermal cycles required for failure). Additionally, three accelerated thermal cycle tests were planned to evaluate the effects of mild, moderate, and severe thermal cycling.

TEST VEHICLES

Components

The five packages utilized in this experiment vary only in pitch and/or body size. Each device is a 64 I/O, daisy chained, 5-layer laminate structure assembled at Universal Instrument's Advanced Process Laboratory.

Each package contains a 0.5mm thick silicon die sandwiched between two 0.4mm thick FR4 substrates using thin layers of underfill to fully encapsulate the die. The ball side substrate contains an 8 by 8 array of solder mask defined (SMD) pads. Each pad has a solderable diameter of 0.381mm and is plated with immersion gold over electrolytic nickel. Solder spheres are attached to the pads through a reflow process using a no-clean tacky flux. The top side substrate is comprised of bare FR4 (i.e. no mask) and is intended to 'balance' the package in order to minimize thermally induced warpage.

In all cases, the silicon die is sized so that all solder bumps are located completely below the die shadow region. Refer to Figure 4 for a drawing of the basic package design and Figure 5 for the component daisy chain.

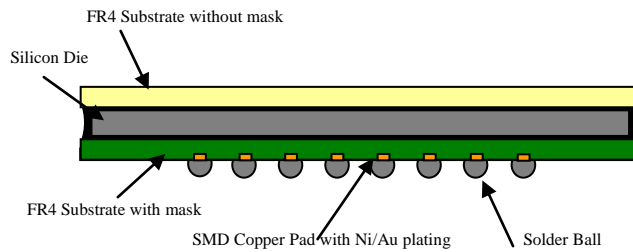


Figure 4. Cross- section of BGA design.

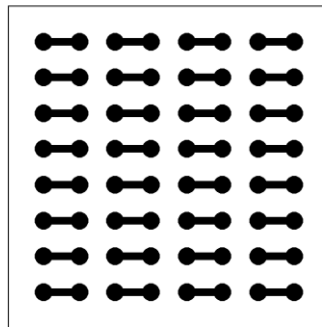


Figure 5. Component daisy chain.

Each package design was constructed using 0.254, 0.30 and 0.40mm diameter solder spheres resulting in a total of 15 variations. The sphere alloy was SAC305. Sphere diameter tolerance was +/- 0.0254mm. Body sizes, die dimensions, maximum DNP and package weights for each package size may be found in Table 1.

Table 1. Component Details.

Pitch	Body Size	Die Size	DNP ¹	Weight ²
1.0mm	14x14mm	12x12mm	4.94mm	0.628g
1.2mm	14x14mm	12x12mm	5.94mm	0.625g
1.4mm	21x21mm	18x18mm	6.93mm	1.418g
1.8mm	21x21mm	18x18mm	8.91mm	1.434g
2.2mm	21x21mm	18x18mm	10.89mm	1.424g

¹ DNP measured from package center to center of corner most solder bump.

² Average weight (in grams) of 30 samples prior to solder ball attachment.

Package CTE was determined using PEMI Moiré interferometry between room temperature and 90°C. The CTE of the package in the attachment pad region is approximately 5.5ppm/°C (Figure 6).

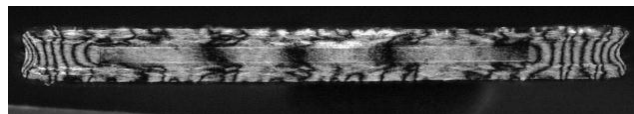


Figure 6. Representative Image used for package CTE measurement. Temperature = 90°C. Number of fringes (U field) = 17.5. Deformation = 417nm/fringe. CTE (in-plane, along the diagonal of the package) = 5.5 ppm/°C.

Package warpage as a function of temperature was evaluated using shadow Moiré imaging. Warpage was measured across the package diagonals at room temperature (Figure 7), 100°C (Figure 8), and then again at room temperature (Figure 9) to simulate the effects of a mild thermal cycle.

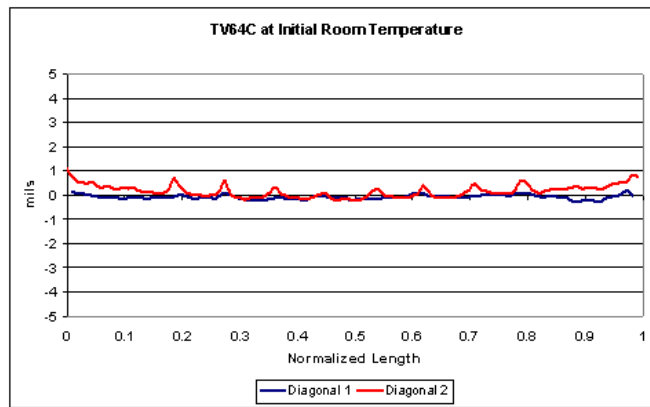


Figure 7. Initial warpage at room temperature (1.8mm pitch sample shown).

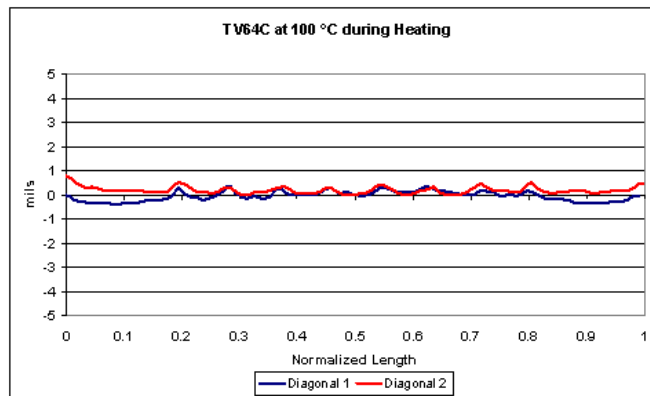


Figure 8. Warpage at 100°C during heating phase (1.8mm pitch sample shown).

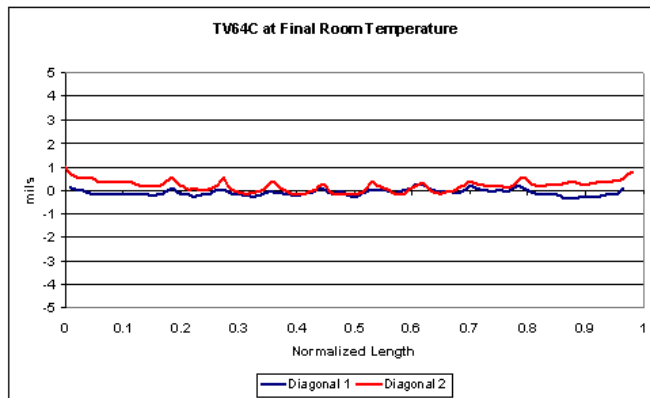


Figure 9. Warpage at room temperature after cooling (1.8mm pitch sample shown).

The shadow Moiré analysis showed that the packages remained flat during thermal excursions between room temperature and 100°C. This indicated that, in the assembled state, the packages would not warp significantly and that in-plane solder joint deformation would most likely be the dominate damage mechanism.

Motherboard

The motherboard used in the experiment was designed to support five samples of each package pitch (25 total) on its top side. The board was a glass fiber reinforced FR4 substrate with four signal layers and a total thickness of 1.575mm. The board contained a copper OSP surface finish. All attachment pads were designed as non-solder mask defined (NSMD) geometries with 0.30mm diameters. Mask openings were 0.40mm in diameter. Surface routing (top and bottom sides) was completed using 1/2oz copper which was plated up to a total thickness of approximately 0.072 mm. Trace widths were approximately 0.10mm. The two internal signal planes were formed using 100% coverage with 1oz copper.

Each assembly site was designed with the same daisy-chain pattern. Only the pad-to-pad pitch was varied. The daisy-chain pattern provided nine probe points which could be used to isolate chain failures to any one row of solder joints as shown in Figure 10.

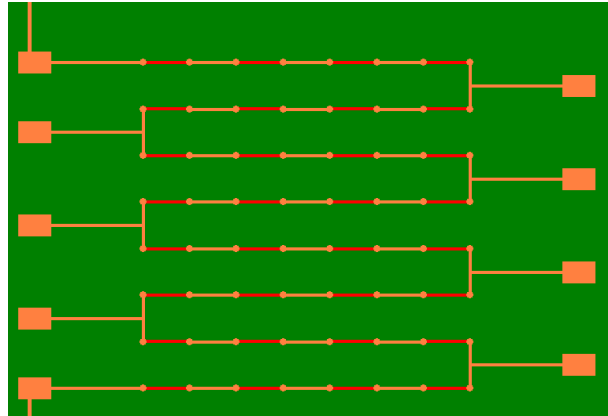


Figure 10. Individual BGA daisy-chain pattern. Orange represents the motherboard connections and red represents the component connections.

Motherboard CTE was determined using PEMI Moiré interferometry between room temperature and 90°C. The CTE of the motherboard within the component footprint region was found to be 14.1ppm/°C (Figure 11).

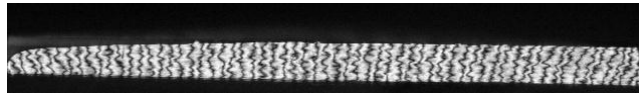


Figure 11. PCB CTE measurement. Temperature = 90°C. Number of fringes (U field) = 60. Deformation = 417nm/fringe. CTE (in-plane, along the length of the sample) = 14.1 ppm/°C.

An image of the motherboard, with packages in place, may be found in Figure 12.



Figure 12. Image of assembled test vehicle.

ASSEMBLY

A flux printing process was used to assemble the components to the motherboards. The flux process was chosen over a paste process in order to minimize solder joint voiding and to maintain a known solder joint volume. The no-clean tacky flux chosen for the assembly process was screen printed over the boards using a 0.1mm thick stencil containing 0.30mm diameter apertures.

The test vehicles were reflow soldered in a forced convection oven containing a nitrogen atmosphere with an oxygen content of less than 50ppm. Temperature profiling indicated that the solder joints reached a peak temperature of 238 to 244°C depending upon their location on the motherboard.

POST ASSEMBLY INSPECTION

The test specimens were inspected after assembly by using an ohm-meter to check electrical continuity and with x-ray imaging to examine solder joint quality. Some samples were excised from the test boards and cross-sectioned to measure solder joint heights and to document the initial solder joint microstructures.

X-ray imaging revealed that an acceptable solder joint formed during the assembly process. No instances of solder bridges or solder balling were observed. Voiding was minimal, and was not expected to be a factor in the experiment. An example x-ray image is found in Figure 13.

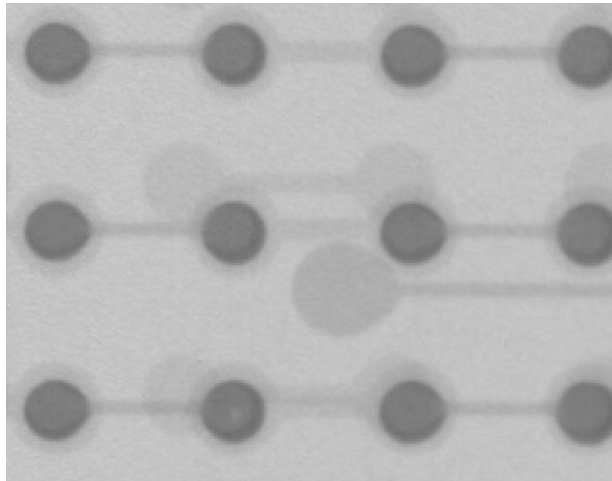


Figure 13. X-ray image of SAC305 solder joints. A small void can be seen in the solder joint located second from left in the bottom row.

Cross-sectioning was performed on a handful of samples in order to examine the solder joint microstructures and to measure standoff heights.

Using a microscope equipped with polarized lenses to view the cross-sections, it appeared that the desired Sn grain structures were obtained. Samples constructed using 0.40mm solder ball diameters always appeared to contain a single grain or beach ball morphology in cross-section while samples created with 0.254mm solder ball diameters most often produced joints which had interlaced twinning. Interestingly, the 0.3mm solder ball diameters most often produced solder joints with the single grain/beach ball morphology, but some joints were found to contain regions in which the Sn grains appeared to be interlaced twinned. Select images of the cross-sectioned solder joints may be found in figures 14, 15 and 16.

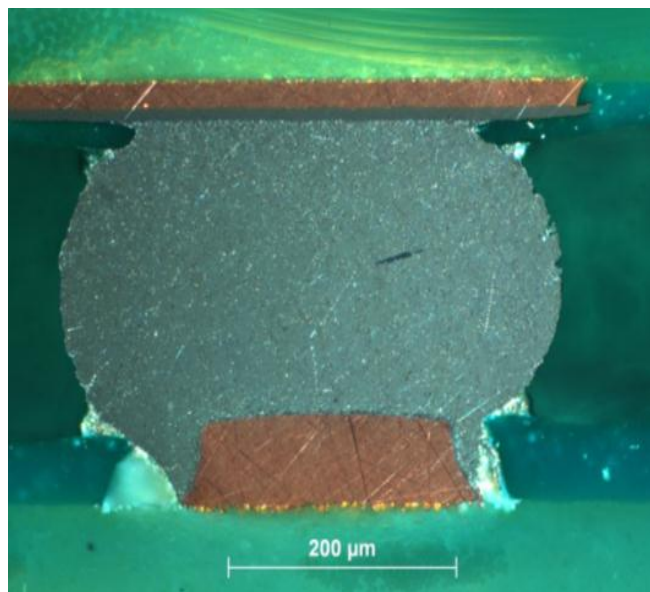


Figure 14. Cross-section of a solder joint created with a 0.4mm diameter solder ball. Cross-polarized lighting indicates that there is a single grain in the cross-sectional view.

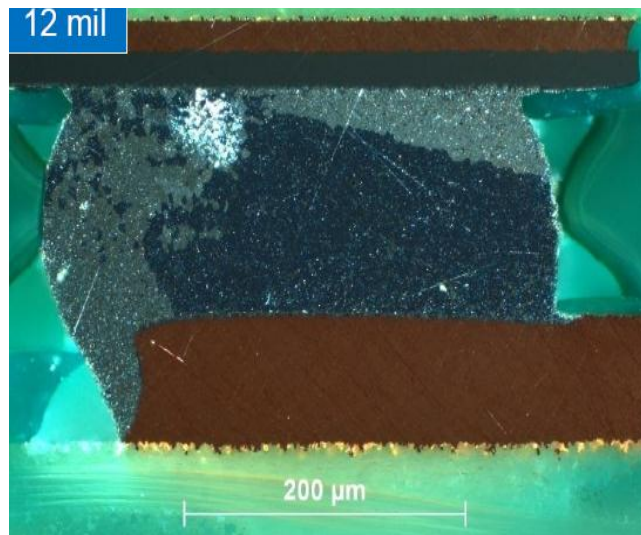


Figure 15. Cross-section of a solder joint created with a 0.3mm diameter solder ball. Cross-polarized lighting indicates that there are two or three large grains in the cross-sectional view as well as a small region of interlaced cyclic twinning at the upper left corner of the joint. A small void is visible near the component attachment pad.

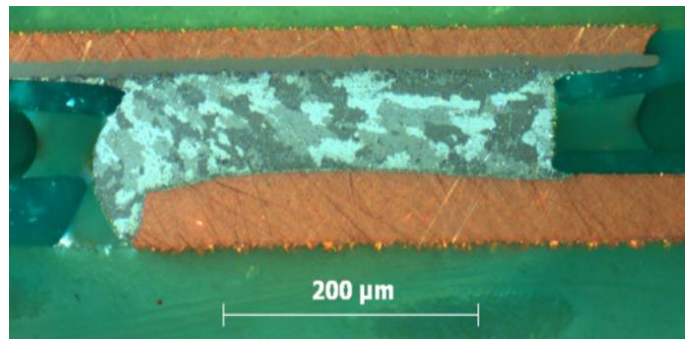


Figure 16. Cross-section of a solder joint created with a 0.254mm diameter solder ball. Cross-polarized lighting indicates that full interlacing of the grain structure has occurred.

Not surprisingly, standoff height was linearly proportional to solder ball diameter. The samples containing 0.254mm solder ball diameters produced solder joints which were about 0.077mm tall and, although 64% taller than our background experiment LGA joints, these samples reasonably represent the upper limits for joint heights expected with LGA assembly. Samples constructed with 0.30mm solder ball diameters resulted in solder joints that were about 0.158mm tall. And samples constructed with 0.40mm solder ball diameters were around 0.255mm tall. Package weight seemed to marginally impact the solder joint height which was expected. The average difference between the standoff heights of the large and small package bodies for a given ball diameter was less than 3%. Solder joint standoff heights are summarized in Table 2.

Table 2. Standoff Height by Body Size and Solder Ball Diameter.

Body Size	Solder Ball Dia.	Standoff Height
14x14mm	0.254mm	0.078mm
14x14mm	0.30mm	0.160mm
14x14mm	0.40mm	0.258mm
21x21mm	0.254mm	0.076mm
21x21mm	0.30mm	0.156mm
21x21mm	0.40mm	0.253mm

ACCELERATED THERMAL CYCLE TESTING

Three accelerated thermal cycle conditions were utilized for this experiment. Each cycle consisted of 10 minute dwell times at the temperature extremes and 9°C per minute transition rates between temperature extremes. The three cycles were:

- 0/100°C
- -20/100°C
- -40/125°C

The test specimens were monitored in-situ using Analysis Tech event detection systems. The detectors were manually set to record resistance spikes (events) exceeding 500 ohms and lasting 200 nanoseconds or longer. Failures were based upon the criteria defined in IPC-9701.

ACCELERATED THERMAL CYCLE TEST RESULTS and ANALYSES

Cycle to failure data was acquired for nearly 100% of the test specimens. Some samples were excised from the circuit boards shortly after failure for additional analysis, but most of the components remained in the chambers until the experiment was concluded.

The failure data was separated by ball diameter, pitch and thermal cycle test conditions and compared using 2-parameter Weibull plots. A summary of the Weibull analyses may be found in Table 3.

Table 3. Summary of Weibull Analyses. N01 is the projected number of cycles for 1% failure occurrence. N63.2 is the number of cycles for 63.2% failure occurrence (also called the characteristic lifetime). Beta is the slope of the straight line fit on a Weibull plot. r^2 is the goodness of the data to a straight line fit.

Ball Diameter (mm)	Pitch (mm)	Temp Cycle (°C)	N01 (cycles)	N63.2 (cycles)	Beta	fit (r^2)
0.254	1.0	0/100	1316	3908	4.228	0.937
0.254	1.2	0/100	511	2509	2.893	0.971
0.254	1.4	0/100	365	1516	3.231	0.902
0.254	1.8	0/100	202	789	3.377	0.918
0.254	2.2	0/100	82	446	2.760	0.957
0.30	1.0	0/100	320	6384	1.538	0.951
0.30	1.2	0/100	170	4266	1.430	0.931
0.30	1.4	0/100	205	699	3.752	0.916
0.30	1.8	0/100	136	404	4.241	0.926
0.30	2.2	0/100	73	303	3.252	0.886
0.40	1.0	0/100	690	4211	2.543	0.970
0.40	1.2	0/100	87	3707	1.227	0.981
0.40	1.4	0/100	4101	1291	4.015	0.838
0.40	1.8	0/100	264	938	3.634	0.955
0.40	2.2	0/100	151	653	3.150	0.896
0.254	1.0	-20/100	880	4386	2.865	0.942
0.254	1.2	-20/100	278	2728	2.016	0.886
0.254	1.4	-20/100	468	1500	3.951	0.983
0.254	1.8	-20/100	141	799	2.654	0.909
0.254	2.2	-20/100	59	380	2.474	0.979
0.30	1.0	-20/100	284	5549	1.549	0.820
0.30	1.2	-20/100	200	5208	1.413	0.950
0.30	1.4	-20/100	144	526	3.556	0.869
0.30	1.8	-20/100	135	350	4.835	0.877
0.30	2.2	-20/100	32	254	2.235	0.949
0.40	1.0	-20/100	711	4244	2.576	0.972
0.40	1.2	-20/100	1265	2984	5.361	0.803
0.40	1.4	-20/100	381	1270	3.822	0.981
0.40	1.8	-20/100	270	802	4.234	0.905
0.40	2.2	-20/100	131	656	2.860	0.940
0.254	1.0	-40/125	339	1917	2.659	0.834
0.254	1.2	-40/125	149	1356	2.085	0.969
0.254	1.4	-40/125	144	815	2.660	0.976
0.254	1.8	-40/125	103	461	3.069	0.926
0.254	2.2	-40/125	28	201	2.359	0.960
0.30	1.0	-40/125	173	2214	1.805	0.979
0.30	1.2	-40/125	115	2002	1.611	0.981
0.30	1.4	-40/125	110	394	3.604	0.918
0.30	1.8	-40/125	66	192	4.314	0.983
0.30	2.2	-40/125	47	172	3.573	0.929
0.40	1.0	-40/125	732	2709	3.517	0.933
0.40	1.2	-40/125	279	1755	2.503	0.968
0.40	1.4	-40/125	216	862	3.325	0.901
0.40	1.8	-40/125	169	474	4.471	0.949
0.40	2.2	-40/125	54	322	2.588	0.979

Recognizing the fact that shear strain increases as solder joint height decreases, one would expect that the reliability of the components assembled with 0.254mm diameter solder spheres would be lower than the reliability of the 0.3 which in turn would be lower than the 0.4mm solder sphere samples. But, when comparing the N63.2 values from Table 3 for the same test temperature and package pitch, there appears to be many exceptions and in fact, there are test groups in which the smallest solder joint survived significantly more thermal cycles than the largest solder joint. Further complicating the analysis is the fact that sometimes the 0.3mm solder ball diameter was more reliable than the either the 0.254 or 0.4mm.

At this point the data seems to confirm the earlier results showing that SAC305 LGAs can be more reliable than SAC305 BGAs, but not for all conditions.

Solving Equation 1 for each test condition and plotting the characteristic lifetime (N63.2) versus the estimated cyclic strain on a log-log plot produces the graphs found in Figure 17.

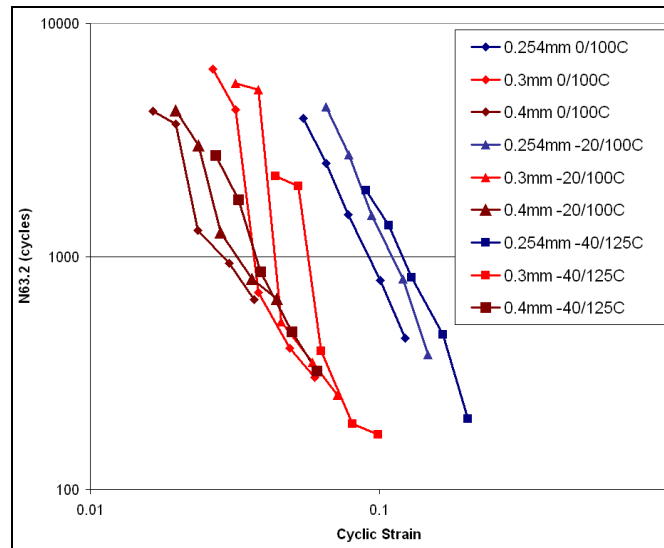


Figure 17. N63.2 versus Cyclic Strain. Data is organized by solder ball diameter and accelerated thermal cycle condition.

When evaluating the lifetime data in this manner it appears that, for a given cyclic strain range, the smallest solder joints formed using 0.254mm ball diameters are more reliable than the solder joints formed by 0.3mm and 0.4mm ball diameters. The notion that smaller solder joints fatigue at a slower rate than larger solder joints subjected to the same strain range has been documented previously by the authors [8], but the current experiment has shown that when identical pad sizes are involved, the actual number of cycles required for the small solder joint (i.e. low standoff height) to fail can be substantially greater than expected.

It also appears that the reliability of the 0.3mm diameter solder joints is similar to that of the 0.4mm diameter solder joints at cyclic strain ranges between 0.05 and 0.1, but at strain ranges lower than 0.05, the 0.3mm diameter solder joints are more reliable. This may indicate that each solder ball size is uniquely sensitive to the strain levels. Similar results have been reported when different solder alloys have been compared (such as SAC305 versus SAC205) [9] and this is simply an extension of the idea to include the same solder alloy containing different Sn grain morphology.

Oddly, Figure 17 shows that for a given cyclic strain range, the -40/125°C thermal test (square data points) actually requires more cycles to produce failures than the -20/100°C thermal test (triangular data points) which in turn requires more cycles to produce failures than the 0/100°C thermal test (diamond data points). These results are not intuitive and why this appears so cannot be explained at this time. However, if the characteristic lifetimes are plotted against the cyclic strain rate, which is computed by dividing Equation 1 by the thermal cycle transition times, the data becomes clear.

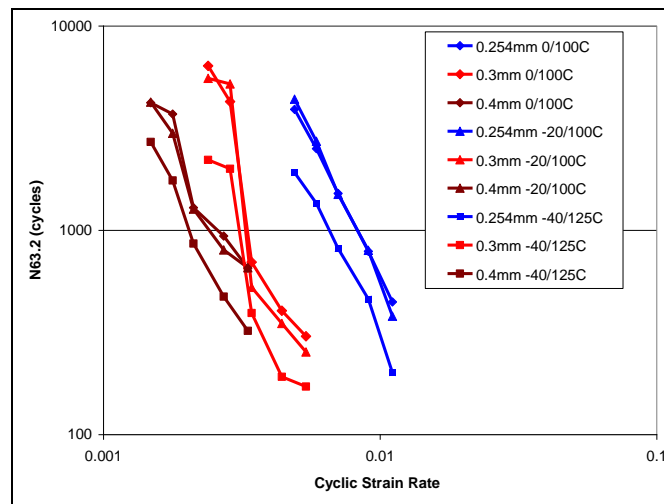


Figure 18. N63.2 versus Cyclic Strain Rate. Data is organized by solder ball diameter and accelerated thermal cycle condition.

Figure 18 indicates that the 0/100°C and -20/100°C accelerated tests require nearly the same number of thermal cycles to produce failure at a given strain rate. This is expected given the similarities in the test conditions and the fact that the lower test temperatures (0°C and -20°C) are believed to be less damaging than the higher test temperature (100°C). Now, for the same strain rate, the -40/125°C test requires significantly fewer cycles to produce failure, which is expected because the total cyclic strain swing is significantly greater and the 125°C test temperature is also more damaging than the 100°C associated with the milder tests.

When comparing the N63.2 results for a single solder ball size in a given thermal cycle test condition it is obvious that increasing DNP by increasing component pitch decreases the number of cycles necessary to produce failure. The trend is predicted by Equation 1 and can be explained by simple mechanics. But the extent of DNP's effect on reliability is not described by the equation. For example, increasing DNP by 20% (from 4.94 to 5.928mm) reduced lifetime by 6 to 35% depending upon the ball size and ATC test condition while a 40% DNP increase (from 4.94 to 6.916mm) reduced lifetime by 57 to 91%. The relative effects of DNP baselined to the 1.0mm pitch device (the most reliable) are provided in Table 4.

Table 4. Reliability Change from 1.0mm Pitch Baseline. N63.2 is in cycles.

Temp Cycle	Ball Dia.	DNP: 4.94mm 5.928mm 6.916mm 8.892mm 10.868mm				
		Pitch: 1.0mm 1.2mm 1.4mm 1.8mm 2.2mm				
		N63.2	% Change from 1.0mm Pitch Baseline			
0/100°C	0.254mm	3908	-36%	-61%	-80%	-89%
0/100°C	0.30mm	6384	-33%	-89%	-94%	-95%
0/100°C	0.40mm	4211	-12%	-69%	-78%	-84%
-20/100°C	0.254mm	4386	-38%	-66%	-82%	-91%
-20/100°C	0.30mm	5549	-6%	-91%	-94%	-95%
-20/100°C	0.40mm	4244	-30%	-70%	-81%	-85%
-40/125°C	0.254mm	1917	-29%	-57%	-76%	-90%
-40/125°C	0.30mm	2214	-10%	-82%	-91%	-92%
-40/125°C	0.40mm	2709	-35%	-68%	-83%	-88%

Examination of Table 4 indicates that a single quantitative effect due to varying DNP (and therefore strain range) may not exist. Instead, each solder ball size appears to have a unique sensitivity to the strain ranges created by varying DNP and ATC parameters. Like the results reported in [9] for different solder alloys, this means that the relative reliability of one solder ball size may change relative to another solder ball size with a change in test or design parameters.

SUMMARY

A strain rate approach for analyzing the ATC reliability data appears to better describe the results than a strain range approach. Using the strain rate approach it has been shown that SAC305 solder joints approximating LGA-like joint qualities (shape, height and microstructure) can be more reliable than larger BGA-like SAC305 solder joints for a given strain rate.

Evidence from this experiment and from literature suggests that the 'small' SAC305 solder joints tend to develop an interlaced twinned Sn grain morphology which has significantly different thermal-mechanical properties than the single grain or beach ball morphology commonly formed in BGA-sized solder joints. These findings suggest that low-profile packages like LGA can be quite reliable in ATC testing –if the proper microstructure forms.

The reason why SAC305 LGA solder joints tend to form the cyclically twinned grain morphology is not well understood. It is known that 'smaller' solder joints tend to undercool more than larger solder joints because less volume means reduced probability for the solidification process to begin (i.e., fewer nucleation sites exist). It is also possible that smaller solder joints cool slower during the reflow soldering process due to reduced surface area. The experiment described in this paper has also found that 'transitional' solder joints containing regions of cyclic twinning and regions of beach ball morphologies can form –especially in intermediately sized solder joints. Components which may have contained these intermediate solder joints performed relatively well at the lower strain rates, but poorly at the higher strain rates.

This experiment has shown that increasing solder joint DNP reduces the ATC lifetime of the solder joint, but a consistent, quantitative result was not obtained. It is possible that each solder joint size has a unique sensitivity to cyclic strain indicating that the relative reliability of one solder ball size to that of another size may change with a change in strain level.

ATC test temperatures have a huge impact on solder joint lifetime. The -40/125°C thermal cycle is significantly more damaging than the -20/100°C and 0/100°C thermal cycle even for the same cyclic strain rate. The -20/100°C and 0/100°C thermal cycle produce similar results especially when comparing similar cyclic strain rates.

Finally, it must be noted that solder joint standoff height is still an important factor in determining component reliability. The notion that increasing standoff height improves reliability by reducing cyclic shear strain is valid as long as material properties remain the same.

ACKNOWLEDGEMENTS

The authors would like to thank Barry Berger, MS '10 and Babak Arfaei, PhD of Binghamton University for their numerous contributions including all aspects of assembly, inspection, testing, data collection/analysis and failure analysis.

REFERENCES

- [1] B. Arfaei, Y. Xing, J. Woods, J. Wolcotts, P. Tumne, P. Borgesen, and E. Cotts, "The Effect of Sn Grain Number and Orientation on the Shear Fatigue Life of SnAgCu Solder Joints", 58th Electronic Components and Technology Conference, 459 (2008).
- [2] B. Arfaei, and E. Cotts "Correlations between the microstructure and fatigue life of near-eutectic Sn-Ag-Cu Pb-free solders" *Journal of Electronic Materials* 38 (2012): 2617-2627.
- [3] L.P. Lehman, Y. Xing, T.R. Bieler, E.J. Cotts, "Cyclic Twin Nucleation in Tin-Based Solder Alloys", *Acta Materialia*, 58, 3546 (2010).
- [4] R. Kinyanjui, L.P. Lehman, L. Zavalij, and E. Cotts, "Effect of sample size on the solidification temperature and microstructure of SnAgCu near eutectic alloys," *J. Mat. Res.* (2011), pp. 2914-2918.
- [5] B. Arfaei, N. Kim, and E. Cotts, "Dependence of the Sn Grain Morphology of SnAgCu Solder on Solidification Temperature" *Journal of Electronic Materials*, (2011)
- [6] A. Qasimeh, Y. Jaradat, L. Wentlent, L. Yang, L. Yin, B. Arfaei and Peter Borgesen, "Recrystallization Behavior of Lead Free and Lead Containing Solder in Cycling", 60th Electronic Components and Technology Conference, 459 (2011).
- [7] B. Arfaei, T. Tashtoush, N. Kim, L. Wentlent, E. Cotts and, P. Borgesen, "Dependence of SnAgCu Solder Joint Properties on Solder Microstructure", 60th Electronic Components and Technology Conference, 1775 (2011).
- [8] Meilunas, M., "Effects of Solder Ball Size on Accelerated Thermal Cycle Testing Results" AREA Consortium 2007.
- [9] Meilunas, M., "2006 Pb-Free Update: Evaluating Accelerated Thermal Test Parameters for Select Solder Alloys" AREA Consortium 2006.